Chinese Journal of
POLYMER SCIENCE

RESEARCH ARTICLE

https://doi.org/10.1007/s10118-023-3053-9
Chinese J. Polym. Sci. **2024**, *42*, 388–399

Particle Distribution Informed by Chain Rigidity in Diblock Copolymer Melts: The Effect of Entropy

Yuguo Chen, Shuanhu Qi*, and Ying Jiang*

School of Chemistry, Beihang University, Beijing 100191, China

Abstract We study the effect of chain rigidity on tailoring the nanoparticle locations for neutral and selective particles embedded in the lamellar morphology formed by semiflexible diblock copolymer chains using self-consistent field calculations. The nanoparticles are modeled through a cavity function, and the semiflexible chains are represented by the continuous Kratsky-Porod chain model. In general situation, the nanoparticles prefer to stay at the interface in order to reduce the interface areas and thus the system free energy. However, the particle distribution at the domain center is subtle, and the underlying physics is intrinsically different depending on the polymer flexibility. In the case of flexible chains, the entropy just contributes a constant shift to the free energy when the nanoparticles move around the domain center indicating that the local metastable state if appears at the domain center is wholly attributed to the local minimum in the enthalpy. If the polymers are rigid, the variation of the particle distribution at the domain center has a close relation with the polymer rigidity and nanoparticle size. In the case of strongly rigid polymers with small nanoparticles, a nearly uniform particle distribution at the domain center is observed, while in other cases, a local enhancement of particle distribution there is found. In contrast to the case of flexible chains, further analysis reveals the crucial role of entropy in controlling the shape of particle distributions at the phase domain. Specifically, the local metastable state appears in the domain center is determined by the large entropy there which arises from the weak coupling of bond orientations that allows the polymer chains to be relatively relaxed. When the particle becomes selective, its distribution in the phase domain exhibits a shift almost uniformly rather than changes its profile, and the underlying physics still holds. In all, our study establishes a strong coupling between the chain rigidity and effect of entropy.

Keywords Semiflexible diblock copolymer; Nanoparticle distribution; Self-consistent field theory; Entropic effect

Citation: Chen, Y.; Qi, S.; Jiang, Y. Particle distribution informed by chain rigidity in diblock copolymer melts: the effect of entropy. *Chinese J. Polym. Sci.* **2024**, *42*, 388–399.

INTRODUCTION

Polymer nanomaterials are a new type of materials formed by nanoscale additives dispersed in a polymer matrix. With the participation of nanoscale additives, polymer nanocomposites can greatly improve their disadvantages in electrical conductivity,[1–4] mechanical strength,[5–8] heat resistance,[9,10] magnetic properties,[11–14] drug delivery[15–18] and other aspects, while preserving the traditional advantages of easy processing and low price. Due to their unique characteristics of appropriate combination, polymer nanocomposites have been studied more and more for their potential applications in real practices.[19–24] Theoretical and experimental studies have demonstrated that the arrangement and distribution of nanoparticles in the polymer matrix are quite relevant to their thermophysical properties of the nanocomposites, which indicates that controlling the morphology of these nanoparticles in the polymer matrix provides a facile and effective way for the design of materials emphasizing specific functions on demand.[25–27] Among different type of polymers forming the matrix, diblock copolymers, which are composed of chemically distinct polymer blocks connected through covalent bonds, have their advantages. Because of the block incompatibility, diblock copolymers are able to self-assemble into various ordered structures,[28–31] and these structures could accommodate the nanparticles at the interfaces or confine them in the bulk regions, therefore regulate the distribution of particles.[32,33] From this respect, a complete understanding of the interplay between nanoparticles and diblock copolymer matrix is definitely necessary and intriguing.

Regarding the hosting of nanoparticles in a diblock copolymer matrix, most of the studies are restricted to flexible Gaussian polymer chains.[34–38] In particular, Matsen *et al*. investigated the distribution of spherical neutral (inert) and selective nanoparticles embedded in the lamellar phase of an incompressible melt consisting of flexible diblock copolymers using self-consistent field (SCF) calculations,[38] and the competition between the locating of nanoparticles at the interface, where the junction points connecting different blocks are situated and the center of the phase domain, where the free ends of polymer chains reside, is illustrated. They found

* Corresponding authors, E-mail: qishuanhu@buaa.edu.cn (S.Q.)
E-mail: yjiang@buaa.edu.cn (Y.J.)

Received September 9, 2023; Accepted September 20, 2023; Published online November 3, 2023

that the neutral nanoparticles always prefer to stay at the interface, where they could reduce the interface area, and hence reach a lowest free energy. Around the domain center, the free energy profile has a plateau, which leads to a uniform particle distribution there. With the particle affinity becoming stronger to one of the species, the free energy of system decreases nearly uniformly for the particles around the corresponding domain center, and finally finds a global minimum there. In this case, the nanoparticle prefers to stay at the domain center. The analysis of the free energy through the partition into contributions from interaction energy and entropy reveals the role of enthalpy and entropy producing the uniform particle distribution in the phase domain. In fact, both the enthalpy and entropy in the domain exhibit a uniform profile, and the flat enthalpy is due to the homogeneous monomer densities around the domain center, while the flat entropy represents the typical characteristic of flexible chains, *i.e.*, polymer conformations are totally free to change in response to the move of nanoparticles making the entropy keep fixed. When the incompatibility between two blocks increases or the incompressible constraint is replaced by the compressible Helfand type of potentials, an interaction energy minimum, and thus a local minimum of the free energy appears at the domain center. This suggests that the interaction energy (enthalpy) rather than entropy dominates the subtle shape of the nanoparticle distribution in the phase domain.

However, the situation becomes different when the matrix chains are rigid. Unlike the flexible case, where the polymer chains could rotate themselves freely, semiflexible (wormlike) diblock copolymers show a strong orientation preference when they are in the lamellar phase, *i.e.*, at the interface, the junction bonds are arranged nearly in perpendicular to the interface, while approaching the phase domain the direction of the chain ends are distributed in a more random manner.[39–41] The weak coupling of the bond orientations at the phase domain promotes the entropy even when a nanoparticle is positioned there, and this could possibly result in a local minimum of the free energy at the domain center. On the other hand, the interaction energy may keep almost unchanged when the nanoparticle moves around the domain center. Such behaviors signify the entropy in tailoring the subtle distribution of nanoparticles in the phase domain formed by semiflexible polymer chains. In fact, the semiflexible chain model becomes popular for the discussion of biological molecules, such as DNA.[42,43] Despite the wide investigation of single-chain conformations and phase behaviors of semiflexible chains,[44–47] the interaction between nanoparticles and semiflexible diblock copolymer matrix remains mostly unexplored, which motivates the interest for further studies.

In this study, we investigate the influence of chain rigidity on the location of neutral and selective nanoparticles in the lamellar phase formed by semiflexible diblock copolymer chains through self-consistent field (SCF) calculations. We found that in the moderately rigid case, although nanoparticles prefer to settle at the interface, a locally metastable state appears at the center of the phase domain for both neutral and selective nanoparticles irrelevant of their size. In the strongly rigid case, nanoparticles still find the stable state at the interface, however, they behave in a different way in the phase domain depending on the size of the nanoparticles. If the particle is small, *e.g.*, much smaller than half of the lamellar period, there is no preference for particles to stay at the domain center, *i.e.*, a local free energy minimum is not observed. On the other hand, when the particle is large, a local minimum of free energy at the domain center appears, which corresponds to a local enhancement in the particle distribution. The profile of nanoparticle distribution for neutral particles shares the same feature with that of selective particles. Further analysis confirms that the entropy rather than the enthalpy which is almost uniform when the particle moves around the domain center, plays the central role in determining the local profiles of the particle distribution at the domain center.

MODEL AND METHODS

The system under consideration contains n linear A/B diblock copolymers and one particle in a volume V with periodic boundaries. All polymer chains are assumed to be identical in structure, *i.e.*, they include the same total number of monomers $N = N_A + N_B$ with N_A (A type monomers) and N_B (B type monomers) of each chain, and have the same monomer volume ρ_0^{-1}, statistical Kuhn monomer length a, persistent length λ, and contour length L. In the following, we will take the monomer length a as the length unit. To introduce the rigidity into the chain, we adopt the Kratky-Porod semiflexible chain model, where one has the relation $a = 2\lambda$ if the bond angles are restricted to small ones. In the present work, we use $L/2\lambda$ to measure the rigidity.[45,46] For example, in the limit of $L/2\lambda$ approaching infinity, the chain recovers fully to a flexible one, while it becomes a rigid rod if $L/2\lambda \ll 1$, and in the intermediate region, the chain behaves like a semiflexible one.

The configuration of the semiflexible chain is characterized by a space curve $\mathbf{R}(s)$, where s ranges from 0 to L parameterizing the contour along the polymer chain. The vector $\mathbf{u} = \mathrm{d}\mathbf{R}(s)/\mathrm{d}s$ defines the local orientation of the contour and $|\mathbf{u}| = 1$. The local orientation introduces a bending energy penalty H_0 for semiflexible chains, which is related to the local curvature $\mathrm{d}\mathbf{u}(s)/\mathrm{d}s$, *i.e.*,

$$H_0 = \frac{\lambda k_B T}{2L}\int_0^1 \mathrm{d}s\left|\frac{\mathrm{d}\mathbf{u}(s)}{\mathrm{d}s}\right|^2 \tag{1}$$

where we have scaled s by the chain length L, and k_B is the Boltzmann constant, T is the temperature. We use f to denote the fraction of A monomers in a chain, so $1 - f$ gives the fraction of B block monomers. In this work, we always assumes that the A/B diblock chain is symmetric, *i.e.*, $N_A = N_B$, then $f = 1/2$. Since the semiflexible chain is inextensible, the energy contribution from local chain stretching does not exist, and this differs from the flexible chains. The nonbonded interaction energy consists of the interplay between different components and a Helfand compressible term, *i.e.*,

$$\begin{aligned}\rho_0^{-1}H_{\mathrm{int}} = &\int d\mathbf{r}\left[\chi_{AB}\hat{\phi}_A\hat{\phi}_B - \chi_{AP}\hat{\phi}_A\phi_P - \chi_{BP}\hat{\phi}_B\phi_P\right]\\ &+\frac{\xi}{2}\int d\mathbf{r}\left[\hat{\phi}_A + \hat{\phi}_B + \phi_P - 1\right]^2\end{aligned} \tag{2}$$

https://doi.org/10.1007/s10118-023-3053-9

where $\hat{\phi}_\alpha$ is the conformation-dependent volume fraction of the α-monomers (α =A, B), which reads $\hat{\phi}_\alpha(\mathbf{r}) = n\rho_0^{-1}\int_0^{f_\alpha} ds\delta[\mathbf{r}-\mathbf{R}(s)]$ with $f_A \equiv f$, and $f_B \equiv 1-f$. Here χ_{AB}, χ_{AP} and χ_{BP} are the so called Flory-Huggins parameters representing the pair interaction strength between A, B monomers and the particle. ξ is a harmonic penalty parameter that quantifies the energy cost for local density deviations. For numerical convergence, we model the particle by a cavity function, which is characterized by a hard core of radius R_P surrounded by a boundary layer of thickness δ. Mathematically, it has the form of

$$\phi_P(\mathbf{r}) = \frac{1}{2} - \frac{1}{2}\tanh\left(\frac{|\mathbf{r}-\mathbf{r}_c| - R_P}{\delta}\right) \tag{3}$$

where $\mathbf{r}_c$ is the central position of the particle, and we normally take $\delta = 0.2a$ in calculation. Please note that the total quantity including polymer chains and the particle is conserved, *i.e.*, $\frac{1}{V}\int d\mathbf{r}(\hat{\phi}_A + \hat{\phi}_B + \phi_P) = 1$. For convenience, we define the following quantities $\chi_P \equiv (\chi_{AP} - \chi_{BP})/2$, $\tilde{\chi}_P \equiv (\chi_{AP} + \chi_{BP})/2$, and $\hat{\phi}_\pm \equiv \hat{\phi}_A \pm \hat{\phi}_B$. The parameter χ_P measures the relative affinity of the particle to A and B monomers, *e.g.*, $\chi_P > 0$ means that the particle adsorbs the A monomers, and on the contrary, $\chi_P < 0$ corresponds to that the particle adsorbs B monomers. In terms of these combinations, we can rewrite the nonbonded interactions as:

$$\rho_0^{-1}H_{int} = \int d\mathbf{r}\left[\frac{\chi_{AB}+2\xi}{4}\hat{\phi}_+^2 - \left(\tilde{\chi}_P\phi_P - \xi(\phi_P-1)\right)\hat{\phi}_+ - \frac{\chi_{AB}}{4}\hat{\phi}_-^2 - \chi_P\hat{\phi}_-\phi_P\right] \tag{4}$$

Using the Hubbard-Stratonovich transform, we would transform the partition function expressed as an integral over particle's degree of freedom $Z = \frac{1}{n!}\prod_{i=1}^{n}\int \mathcal{D}\mathbf{R}_\alpha(s)\,\mathcal{D}\mathbf{u}_\alpha(s)\exp(-\beta(H_0+H_{int}))$ into that as an integral over continuous fields, *i.e.*, $Z = \int \mathcal{D}\omega_+\,\mathcal{D}\omega_-\exp[-C\bar{\phi}VF(\omega_+,\omega_-,\mathbf{r}_c)]$ with the free energy functional

$$F(\omega_+,\omega_-,\mathbf{r}_c) = \frac{1}{\bar{\phi}V}\int d\mathbf{r}\left[\frac{\omega_-^2}{N\chi_{AB}} - \frac{2N\chi_P}{N\chi_{AB}}\phi_P\omega_- + \frac{\omega_+^2 - 2N\xi\phi_+ i\omega_+}{N\chi_{AB}+2N\xi}\right] - \frac{1}{V}\ln Q \tag{5}$$

where the prefactor $C \equiv \rho_0 R_g^3/N$, R_g is the mean radius of gyration of an ideal polymer containing N monomers, and $\bar{\phi} = \frac{1}{V}\int d\mathbf{r}\phi_+(\mathbf{r})$ gives the average volume fraction of polymer chains. The free energy F gives the free energy per chain. The field ω_α ($\alpha = +,-$) is the auxiliary potential conjugated to the volume fraction field ϕ_α. It is obviously that ω_α is only a function of the position $\mathbf{r}$ independent of the orientation variable $\mathbf{u}$. The single chain partition function Q is expressed as $Q = \frac{1}{4\pi V}\int \mathcal{D}\mathbf{R}(s)\,\mathcal{D}\mathbf{u}(s)\exp[-\beta H_0 - \int_0^f ds\omega_A(\mathbf{R}(s)) - \int_f^1 ds\omega_B(\mathbf{R}(s))]$, where $\omega_A \equiv i\omega_+ - \omega_-$ and $\omega_B \equiv i\omega_+ + \omega_-$ define the auxiliary potentials conjugated to ϕ_A and ϕ_B, respectively. To obtain the SCF equations, we perform the saddle-point approximation by extremizing the free energy F with respect to the functional variables $i\omega_+$ and ω_-, and obtain

$$\begin{aligned} -\phi_A + \phi_B + \frac{2\omega_- - 2N\chi_P\phi_P}{N\chi_{AB}} &= 0 \\ \phi_A + \phi_B - \frac{2i\omega_+ + 2N\xi\phi_+}{N\chi_{AB}+2N\xi} &= 0 \end{aligned} \tag{6}$$

The volume fraction ϕ_A and ϕ_B relate the fields ω_A and ω_B through the end-integrated propagators $q(\mathbf{r},\mathbf{u},s)$ and $q^\dagger(\mathbf{r},\mathbf{u},s)$ as

$$\begin{aligned} \phi_A &= \frac{\bar{\phi}}{4\pi Q}\int d\mathbf{u}\int_0^f ds q(\mathbf{r},\mathbf{u},s)q^\dagger(\mathbf{r},\mathbf{u},s) \\ \phi_B &= \frac{\bar{\phi}}{4\pi Q}\int d\mathbf{u}\int_f^1 ds q(\mathbf{r},\mathbf{u},s)q^\dagger(\mathbf{r},\mathbf{u},s) \end{aligned} \tag{7}$$

The forward propagator $q(\mathbf{r},\mathbf{u},s)$ and backward propagator $q^\dagger(\mathbf{r},\mathbf{u},s)$ satisfy respectively the following modified diffusion equations (MDE)

$$\begin{aligned} \frac{\partial q(\mathbf{r},\mathbf{u},s)}{\partial s} &= \left[\frac{L}{2\lambda}\nabla_{\mathbf{u}}^2 - L\mathbf{u}\cdot\nabla_{\mathbf{r}} - \omega(\mathbf{r},s)\right]q(\mathbf{r},\mathbf{u},s) \\ \frac{\partial q^\dagger(\mathbf{r},\mathbf{u},s)}{\partial s} &= \left[-\frac{L}{2\lambda}\nabla_{\mathbf{u}}^2 + L\mathbf{u}\cdot\nabla_{\mathbf{r}} - \omega(\mathbf{r},s)\right]q^\dagger(\mathbf{r},\mathbf{u},s) \end{aligned} \tag{8}$$

with different initial conditions $q(\mathbf{r},\mathbf{u},0) = 1$, and $q^\dagger(\mathbf{r},\mathbf{u},1) = 1$. Here the potential $\omega(\mathbf{r})$ is defined as $\omega \equiv \omega_A$ for $0 \le s \le f$, and $\omega \equiv \omega_B$ for $f < s \le 1$. In terms of the forward propagator, the single chain partition function Q can be written as $Q = \frac{1}{4\pi V}\int d\mathbf{r}\int d\mathbf{u}q(\mathbf{r},\mathbf{u},1)$.

The unknown field variables are ϕ_A, ϕ_B, $i\omega_+$, ω_-, then the Eqs. (6)–(8) make a closed form when the particle is fixed at some position in the system and these equations are solved numerically. In the 3-dimensional (3d) space the propagators $q(\mathbf{q},\mathbf{u},s)$ and $q^\dagger(\mathbf{r},\mathbf{u},s)$ contain six variables, which are computationally very expensive. To facilitate the numerical calculation, in the present study, we consider a cylindrical particle immersed in the lamellar phase, and then the geometric symmetry of the system simplifies the calculation to 2d spatial space (xy) and 1d orientational space θ (see Fig. 1). The y-axis is aligned in parallel to the normal of the A/B interface, and the polar angle θ is defined as the angle between the bond vector $\mathbf{u}$ and the axis y. The propagators become a function of x, y, θ, and the contour variable s. The MDEs are solved by the method of combining spherical harmonic basis and Fourier basis expansion,[39,48,49] where in the spacial space 512×512 basic modes are chosen when performing fast Fourier transformation, and in the polar direction, 25 basis functions are adopted for the Legendre transformation. The SCF equations are solved iteratively treating $i\omega_+$ and ω_- as the variables using the simple mixing scheme for the first 50 steps to start the iteration and later the Anderson mixing scheme[50,51] to reach efficiently the convergent state. The iteration procedure stops if the magnitude of difference of $i\omega_+$ and ω_- at each collocation point in two successive steps is smaller than 10^{-6}.

The main concern of the paper is the influence of the chain rigidity on the particle distribution in the lamellar phase. To tune the rigidity of diblock copolymer chains, we take several values of $L/2\lambda$ covering the range from $L/2\lambda = 1$ to $L/2\lambda = 100$ indicating that the chain varies from quite rigid to flexible. Since the persistence λ is normally fixed for polymers with specific chemical components and topological struc-

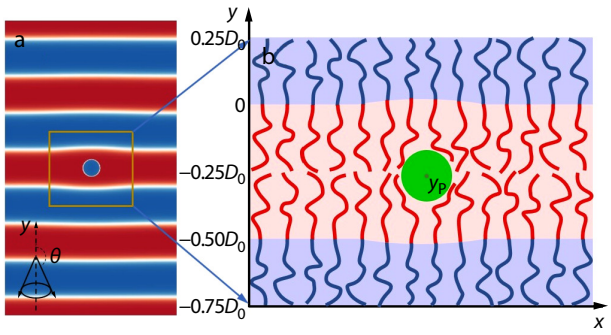

Fig. 1 Illustration of the lamellar morphology of the system involving one particle: the volume fraction distribution of the B block monomers (a) and the corresponding schematic representation for the particle embedded in the B domain of the lamellar phase within one period D_0 (b). The normal of the A/B interface aligns in parallel to the y axis, and y_P denotes the y-coordinate of the particle center. The polar angle θ is defined as the angle between the bond vector $\mathbf{u}$ and the axis y. The A block is colored in blue, while the B block is colored in red.

tures, one then could select the flexibility be choosing different chain length L. However, it should be noted that the flexibility is relative depending on the properties under consideration. For example, the chain can be viewed as moderately semiflexible when studying the particle distributions while completely flexible or highly semiflexible in other situations. We fix the parameters $N\chi_{AB} = 25$ and $N\xi = 1000$ such that in all cases of chains with different rigidity the diblock copolymer melt can form a lamellar phase. To obtain the particle distribution what we really calculate is the free energy F as a function of the particle position $\mathbf{r}_c = (x_c, y_P)$. Since the lamellar phase is homogeneous along the x direction, the free depends only on y_P, *i.e.*, $F = F(y_P)$. Also the A and B block chains are symmetric to the particle, we only set y_P to locate at the interface and in the B domain region. In the present work, we take the free energy for particles at the interface F_0 as the reference, then the particle distribution can be expressed as

$$P(y_P) \propto \exp[-\Delta F(y_P)] \tag{9}$$

where $\Delta F(y_P) = F(y_P) - F_0$. The chain rigidity in the present work is characterized by the ratio of contour length to twice the persistence length ($L/2\lambda$), and the contour length is fixed at $50a$, so, when λ changes, the lamellar period also changes, which means that the relative location and relative size of the particle become different. The coupling between chain rigidity and lamellar period complicates the analysis of the influence of the chain flexibility and particle size on the particle distributions. To overcome this problem, we use the ratio of particle diameter d_P over half of the lamellar period D_0 to define the particle size. In this case, the chain rigidity $L/2\lambda$ and particle size $d_P/0.5D_0$ are treated as two independent parameters, and y_P/D_0 specifies the location of the particle. Hence, the size and location in this work are all relative values defined with respect to the lamellar period. In real calculation, the box size along y direction is set large enough involving 4 lamellar periods and the particle moves around the center of the system that the size effect of the system is negligibly small (see Fig. 1).

The phase morphology of the system is characterized by the volume fractions ϕ_A and ϕ_B, and chain conformations are extracted from the propagators $q(\mathbf{r}, \mathbf{u}, s)$ and $q^\dagger(\mathbf{r}, \mathbf{u}, s)$. For example, one calculates the probability of finding the chain end at position $\mathbf{r}$ through

$$P_{end}(\mathbf{r}) = \frac{\bar{\phi}}{4\pi Q}\int d\mathbf{u} q(\mathbf{r}, \mathbf{u}, 1) \tag{10}$$

To see the influence of particles on the chain orientation, we focus on the B block part (as the particle moves between the A/B interface and the B domain region), and define an average orientation $\bar{\mathbf{u}}(\mathbf{r})$ showing the average orientation of the polymer chain at position $\mathbf{r}$. It reads

$$\bar{\mathbf{u}}(\mathbf{r}) = \frac{\bar{\phi}}{4\pi Q}\int d\mathbf{u}\int_0^1 ds q(\mathbf{r}, \mathbf{u}, s) q^\dagger(\mathbf{r}, \mathbf{u}, s) \tag{11}$$

The magnitude of the vector $\bar{\mathbf{u}}(\mathbf{r})$ measures the strength of orientation at certain direction at position $\mathbf{r}$. The limiting case $|\bar{\mathbf{u}}(\mathbf{r})| = 0$ means that all bonds at $\mathbf{r}$ do not have any orientation preference. On the contrary, $|\bar{\mathbf{u}}(\mathbf{r})| = 1$ indicates that all bonds at position $\mathbf{r}$ have the same direction.

To understand the basic mechanism that controls the free energy difference ΔF, we split the free energy into contributions from enthalpy (interactions) and entropy, *i.e.*, $\Delta F(y_P) = \Delta U(y_P) - T\Delta S(y_P)$, where $\Delta U(y_P) = U(y_P) - U_0$ is the enthalpy difference, $\Delta S(y_P) = S(y_P) - S_0$ being the entropy difference, and the subscript 0 means that the values are obtained at the A/B interface. In terms of the fields and single chain partition function, the enthalpy and entropy can be expressed as

$$\begin{aligned} U(y_P) &= \frac{1}{\bar{\phi}V}\int d\mathbf{r}\Big[N\chi_{AB}\phi_A\phi_B - N\chi_P(\phi_A - \phi_B)\phi_P \\ &\quad + \frac{\xi}{2}(\phi_A + \phi_B + \phi_P - 1)^2\Big] \\ S(y_P) &= \frac{1}{\bar{\phi}V}\int d\mathbf{r}\Big[\phi_A\omega_A + \phi_B\omega_B\Big] + \frac{1}{V}\ln Q \end{aligned} \tag{12}$$

RESULTS AND DISCUSSION

According to Eq. (9), the particle distribution can be specified by the free energy difference, so in the following we mainly focus on the free energy difference, and to completely examine the effect of chain rigidity, we would compare the free energy with different chain flexibility $L/2\lambda$, particle size $d_P/0.5D_0$, and particle selectivity $N\chi_P$. One should note that the free energy F has the meaning of energy per chain, so the comparison of the magnitude of F with different chain flexibility is meaningless since the persistence length in these cases is different. What we are more interested is the free energy difference when the particle moves in the lamellar phase, and this reveals the tendency of the particle where they would like reside in the system. Let's get started with the case of a neutral particle, *i.e.*, $N\chi_P = 0$.

A Neutral Particle

We first consider a small particle $d_P/0.5D_0 = 0.14$ and plot in Fig. 2 the free energy as well as its contributions as a function of the particle location. Fig. 2(d) clearly demonstrates that in all cases the particle prefer to stay at the interface $y_P/D_0 = -0.5, 0$ because a global free energy minimum is obtained there, while the shape of the free energy profile and thus the corresponding curve of particle distribution strongly depend on the chain flexibility. For example, in the case of flexible chains ($L/2\lambda = 100$), the free energy shows a small minimum around $y_P/D_0 = -0.25$

https://doi.org/10.1007/s10118-023-3053-9

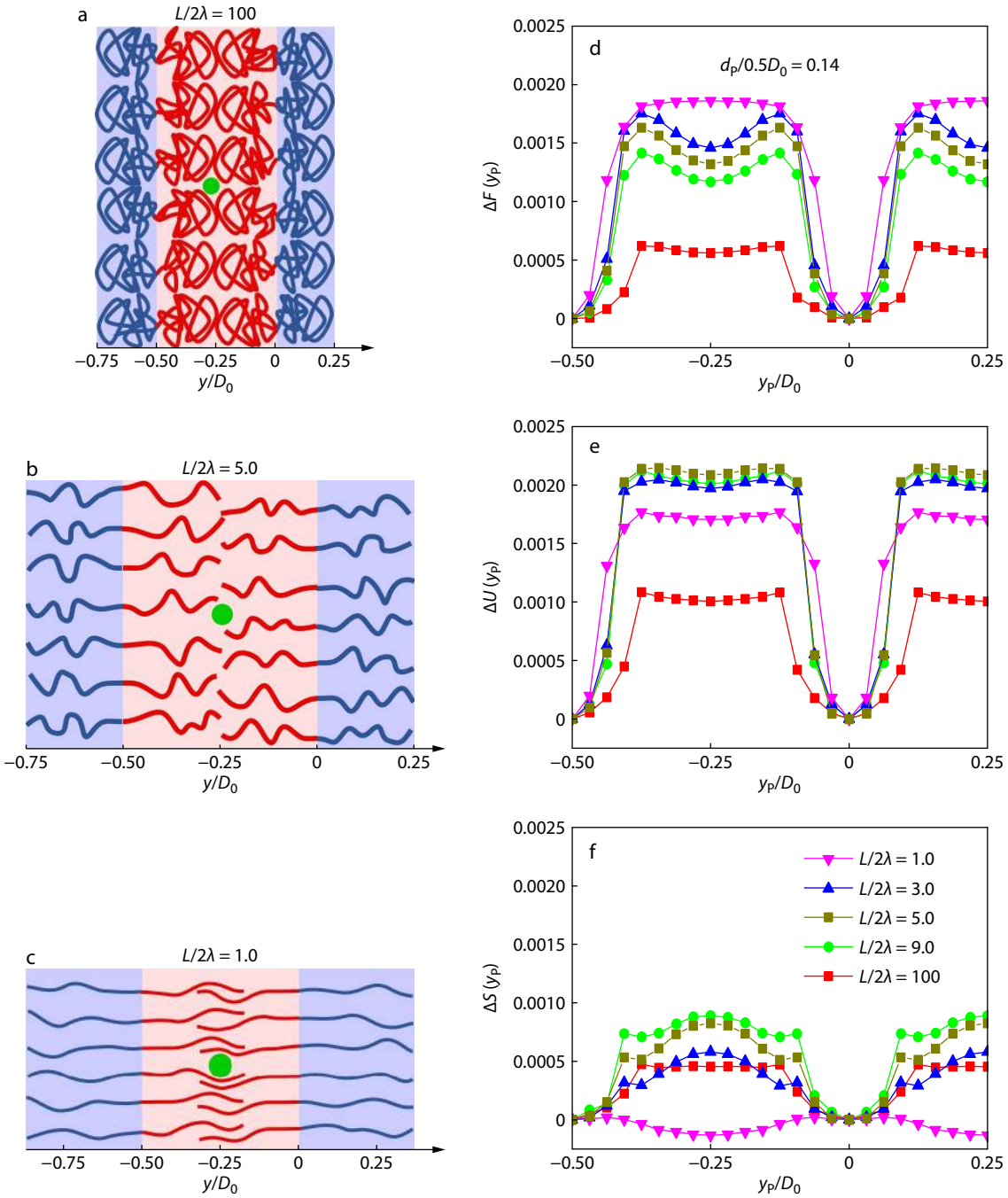

Fig. 2 Schematic representation of a small particle immersed in the lamellar phase formed by flexible (a), moderately semiflexible (b), and strongly semiflexible (c) diblock copolymer chains and the free energy (d), enthalpy (e), and entropy (f) distribution as a function of particle location with different chain flexibility ranging from flexible $L/2\lambda = 100$ to strongly semiflexible $L/2\lambda = 1.0$. The particle has a size of $d_P/0.5D_0 = 0.14$ with particle selectivity $N\chi_P = 0.0$. The legends in (f) refer to all three panels (d), (e), and (f).

indicating that there is weak preference for the particle to stay at the domain center. Please note that this is different from the totally incompressible system, where for small particles the free energy is nearly a constant around the domain center, for further details we refer the reader to Ref. [38]. On the other hand, for the strongly semiflexible chains $L/2\lambda = 1.0$, the particle kind of hates to stay at the domain center, because the free energy seems to slightly increase approaching the domain center. In contrast, when the polymer chains are moderately semiflexible, the free energy exhibits a local minimum at the domain center, which corresponds to a metastable state there for the particle. The minimum reaches a lowest value around $L/2\lambda \simeq 5.0$. The particles located at the domain center being metastable means that they have large probability to move to the interface which is the stable location. The life time of the metastable state is related to the free energy barrier between these two states, and it

https://doi.org/10.1007/s10118-023-3053-9

would be practically useful if the life time is sufficiently long.

The free energy analysis by partitioning the free energy into contributions from enthalpy and entropy demonstrates different mechanisms controlling the free energy profile around the domain center. If the polymers are flexible, Fig. 2(f) shows that the entropy is almost independent of the particle locations around $y_P/D_0 = -0.25$ suggesting that the weak minimum found there is attributed mainly from the enthalpy, and this is confirmed by the shallow minimum in the interaction energy curve shown in Fig. 2(e) (see the red line). On the contrary, when the polymers are semiflexible, both in the cases of moderately semiflexible chains and strongly semiflexible chains, the entropic part changes relatively dramatic compared to the enthalpy in the phase domain, which signifies the dominance of entropy in tailoring the free energy profile. The difference is at the domain center for moderately semiflexible chains, the entropy maximum tends to bound the particle there, while for strongly semiflexible chains, the entropy minimum would push the particle away.

The entropic behavior of the particle immersed in the phase domain is closely related to the extent to which the particle disturbs the chain conformations. For flexible polymers, unlike the junction point which is a bit fixed at the interface, the chain end is completely free. When the particle moves around the domain center (*i.e.*, near the free chain ends), the polymer chain is able to tune its conformation that it is hardly stretched or suppressed, and this explains the result that the entropy for the case of the flexible chain is almost independent of the particle location in the domain (see the red curve in Fig. 2f). On the other limit of strongly semiflexible case, the stiff ends may interpenetrate each other, and when the particle is put at the domain center, it compresses a bit of the polymer chains. Such behavior can be illustrated in Fig. 3(b) where the free ends are relatively aggregated just above and below the particle. In contrast, the free end distribution is not quite disturbed when the particle is located at the interface (see Fig. 3a). Such difference leads to the smaller entropy at the domain center. It may be noted that the free energy dip at the domain center is very shallow, and could be treated flat from the point of relative magnitude. However, the physical effect is definite, at least it does not tend to attract particles to the domain center. This is different from the case of moderately semiflexible chains, where relatively free chain ends and weak orientation of chain bonds at the domain center result in a higher entropy for the particle located there (see for example the curve for $L/2\lambda = 5.0$ in Fig. 2(f), the figure for the free end distribution is not presented).

Now we consider a large particle with $d_p/0.5D_0 = 0.46$ and plot in Fig. 4 the free energy and its contributions as a function of particle location. Similar to the case of a small particle, the large particle also prefers to stay at the interface $y_P/D_0 = -0.5, 0$, as a global free energy minimum is obtained there. At the center of the phase domain, a metastable state

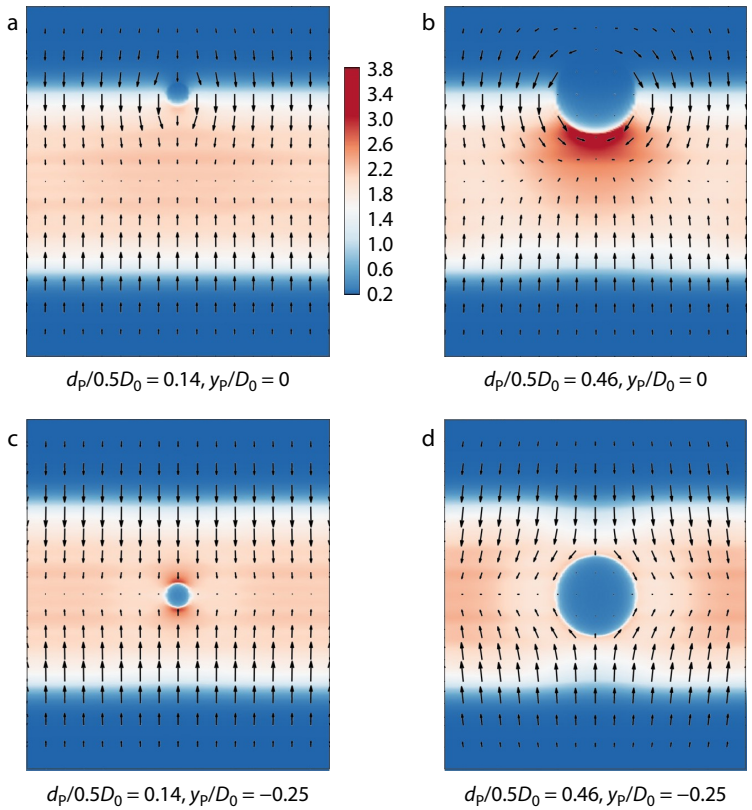

Fig. 3 Distribution of the B chain end location $P_{end}(\mathbf{r})$ and average orientation $\bar{\mathbf{u}}(\mathbf{r})$ of the polymer chain with $L/2\lambda = 1.0$ around the particle for small particle at (a) interface ($y_P/D_0 = 0$) and (b) the domain center ($y_P/D_0 = -0.25$), for large particle at (c) interface ($y_P/D_0 = 0$) and (d) the domain center ($y_P/D_0 = -0.25$).

https://doi.org/10.1007/s10118-023-3053-9

corresponding to the local free energy minimum appears for all the situations of the chain rigidity ranging from flexible $L/2\lambda = 100$ to strongly semiflexible $L/2\lambda = 1.0$. This is different from the case of a small particle, where a local free energy maximum rather than a minimum is observed for strongly semiflexible chains at the domain center. This result indicates that when the particle becomes sufficiently large, a metastable state at the domain center always appears independent of the chain rigidity.

The analysis of the free energy contributions confirms the same underlying mechanism as that for a small particle controlling the particle distributions in the domain region, *i.e.*, for flexible chains the enthalpy dominates, while for semiflexible chains the entropy is responsible. For example, for flexible chains with $L/2\lambda = 100$, the entropy is uniform around $y_P/D_0 = -0.25$ (see Fig. 4f), therefore the minimum shown in

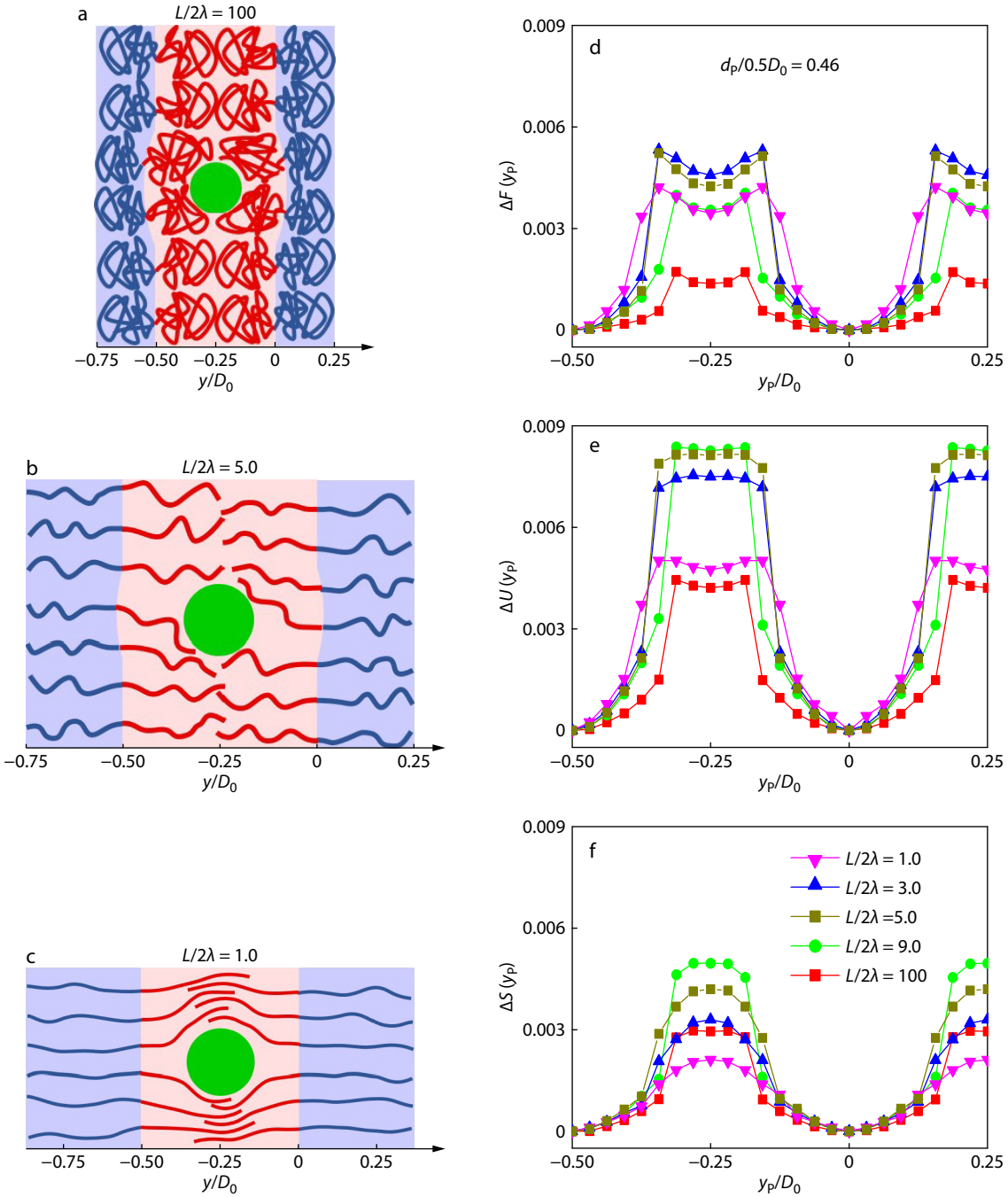

Fig. 4 Schematic representation of a large particle immersed in the lamellar phase formed by flexible (a), moderately semiflexible (b), and strongly semiflexible (c) diblock copolymer chains and the free energy (d), enthalpy (e), and entropy (f) distribution as a function of particle location with different chain flexibilities ranging from flexible $L/2\lambda = 100$ to strongly semiflexible $L/2\lambda = 1.0$. The particle has a size of $d_P/0.5D_0 = 0.46$ with particle selectivity $N\chi_P = 0.0$. The legends in (f) refer to all three panels (d), (e), and (f).

https://doi.org/10.1007/s10118-023-3053-9

the free energy there arises from the minimum in the interaction energy (see Fig. 4e). In contrast, for semiflexible chains, the interaction energy varies more gently than the entropy in the phase domain, and the sharp maximum of entropy results in the local free energy minimum at the domain center. It should be noted that the entropy always reaches a maximum at the domain center irrelevant to the chain rigidity, which is different from the case of a small particle, where for strongly semiflexible chains, the entropy has a minimum at the domain center.

The entropic behavior for a large particle immersed in the phase domain can also be explained by the extent to which the particle disturbs the conformations. For flexible chains, the free ends can always get relaxed if the particle moves a bit around the domain center, and the chains are not stretched or compressed at all, thus the entropy is independent of the particle location in the phase domain. For strongly semiflexible chains, the inserted large particle disturbs the conformation of polymer chains in a different way than that of a small particle as can be seen from the comparison between Figs. 3(a) and 3(b) and Figs. 3(c) and 3(d). When a large particle is at the interface, we found an enhanced chain end distribution near the particle surface (see Fig. 3c), which represents the gathering of polymer chain ends there, and this is an indication that polymer chains are stretched around the lower side of the particle. The stretching of polymer chains would decrease the conformational entropy. While at the domain center, the free end distribution around the particle is relatively uniform meaning that polymer conformations are not strongly altered (see Fig. 3d). Such behavior is consistent to the observation that for a large particle immersed in strongly semiflexible chains, the system has a small entropy when the particle is at the interface compared to that at the domain center. Similar behaviors hold in the case of moderately semiflexible chains, which also predicts an entropy maximum at the domain center (see for example the curve corresponding to $L/2\lambda = 5.0$ in Fig. 4f, and the free end distribution is not shown).

A Selective Particle

In this section, we investigate the influence of particle selectivity on its distributions, and without loss of generality, we assume that the particle adsorbs B monomers and repels A monomers, *i.e.*, we always set $N\chi_P < 0$, and the larger magnitude of $|N\chi_P|$ the stronger particle selectivity.

Fig. 5 plots the free energy, enthalpy, and entropy of the system as a function of particle location with different chain rigidity and particle selectivity of for the case of a small particle $d_P/0.5D_0 = 0.14$. One major feature of the free energy distribution correlated to particle selectivity is that the system free energy shift roughly in a uniform manner when the particle is located in the phase domain by increasing the particle selective strength. This is clearly seen in Figs. 5(a), 5(d), and 5(g), *i.e.*, around $y_P/D_0 = -0.25$ in the B phase domain, the free energy increases with increasing the selective strength, while around the $y_P/D_0 = 0.25$ in the A phase domain, the free energy decreases with increasing the selective strength. This indicates that the particle selectivity mainly shifts the particle distribution as a whole rather than changes the distribution profile in the phase domains (especially around the domain center). When the selectivity becomes sufficiently strong, for example, $N\chi_P = -6.0$ for flexible chains $L/2\lambda = 100$ (see Fig. 5a), the free energy at the B domain becomes smaller than that at the interface meaning that the particle prefers to stay at the domain rather than at the interface. For semiflexible chains $L/2\lambda = 5.0$ and $L/2\lambda = 1.0$, a global free energy minimum at the domain center is not observed. However, the tendency is clear, *i.e.*, with the increase of particle selectivity, the free energy at $y_P/D_0 = -0.25$ becomes smaller, and a global minimum should be expected if $|N\chi_P|$ is large enough.

To investigate the underlying physics, we also partition the free energy into contributions from enthalpy and entropy. For flexible chains, Fig. 5(b) shows clear enthalpy minimum at $y_P/D_0 = -0.25$ the domain center for the neutral particle ($N\chi_P = 0$), and the minimum dip become weaker with increasing the particle strength selectivity. On the other hand, the entropy profile is almost flat in the domain region in the case of a neutral particle. When the strength of the particle selectivity increases, the entropy in the domain region as a whole is promoted with the flat region becoming narrow. Such behaviors of enthalpy and entropy change with the introduction of particle selectivity suggest that the free energy minimum at the domain center if exists arises mainly from the minimum appears in the enthalpy, and this is true for both neutral and selective particles. For semiflexible chains, however, it is easy to find in Fig. 5 that the subtle distribution of free energy in the phase domain is controlled by the entropy rather than the enthalpy. In the case of moderately semiflexible chains, Fig. 5(e) shows that the enthalpy profile is roughly flat in the phase domain for neutral and selective particles, and thus the free energy minimum at $y_P/D_0 = -0.25$ comes from the entropy maximum there. The entropy maximum can be explained by the weaker bond orientation of the free chain ends. In contrast, in the case of strongly semiflexible chains, the free energy at $y_P/D_0 = -0.25$ for any $N\chi_P$ is nearly flat or maybe a bit humped, which definitely correlates to the entropy minimum there, as it overcompensates the weak enthalpy declining. The entropy minimum appeared at $y_P/D_0 = -0.25$ is related to the spacial confinement caused by the interpenetration of chain ends as discussed previously. It should be noted that for semiflexible chains, with the increase of particle selective strength, the enthalpy continuously changes, while the entropy profile settles onto a single curve independent of $N\chi_P$. In all, the partition of free energy into enthalpy and entropy demonstrates that the introduction of particle selectivity does not bring any new physics in determining the particle distributions, *i.e.*, still the particle distribution around the domain center is determined by the enthalpy for flexible chains, and by the entropy for semiflexible chains.

Fig. 6 shows the free energy of the system and its components as a function of particle location with different chain rigidities and particle selectivities for the case of a large particle $d_P/0.5D_0 = 0.46$. In all the cases, we find the global free energy minimum at the interface and local minimum at the domain center, meaning that the most probable location in the system for the particle to stay is the interface, and it is just metastable if the particle stays at the domain center. With the promotion of particle selectivity to B monomers, the profile of

https://doi.org/10.1007/s10118-023-3053-9

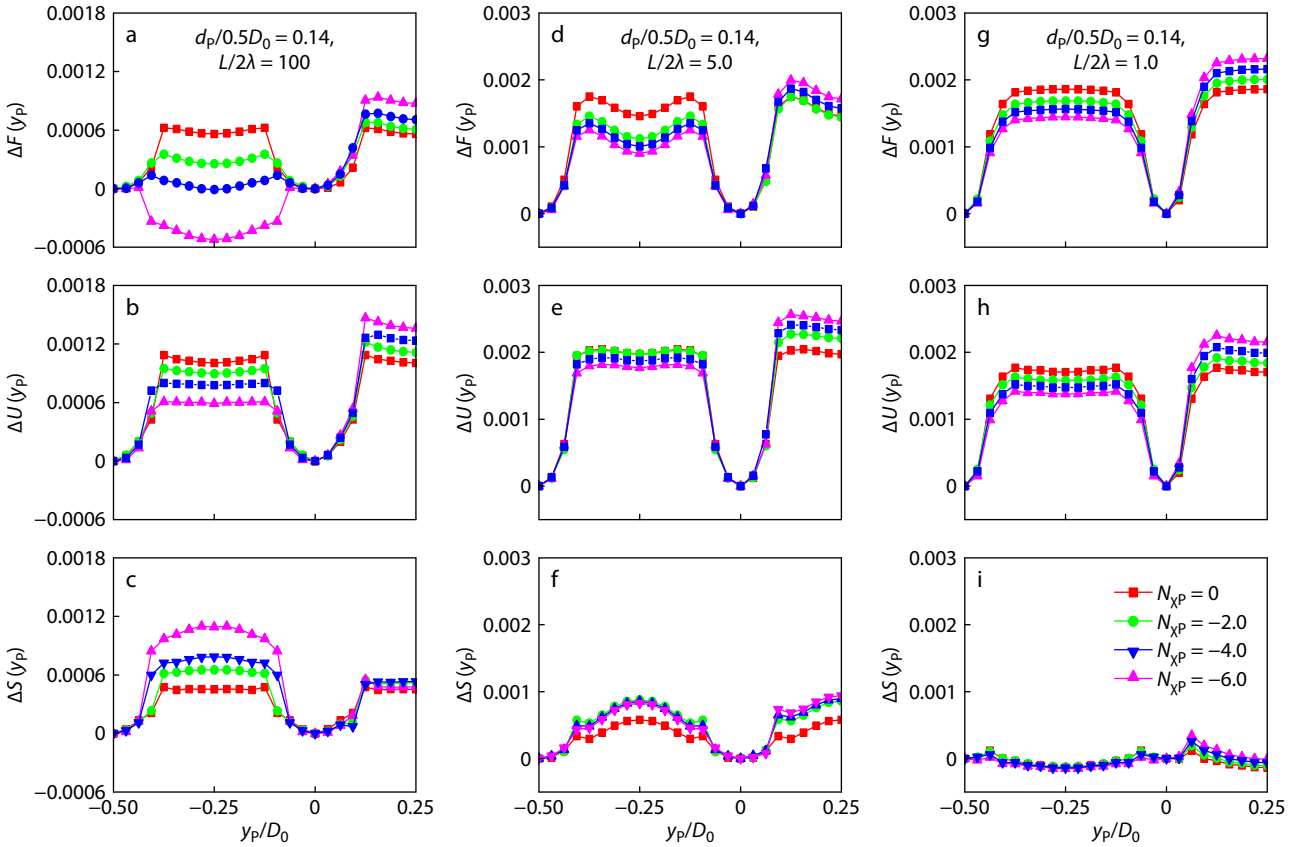

Fig. 5 The distribution of free energy, enthalpy and entropy for flexible chains $L/2\lambda = 100$ (a, b, c), moderately semiflexible chains $L/2\lambda = 5.0$ (d, e, f), and strongly semiflexible chains $L/2\lambda = 1$ (g, h, i). The particle has a small size of $d_P/0.5D_0 = 0.14$ with the particle selectivity denoted, and $N\chi_P < 0$ means that the particle adsorbs B monomers and repels A monomers. The legends in (i) are identical and they refer to all other panels.

free energy becomes asymmetric with its value within the B domain being reduced and that within the A domain increased. Therefore, a global free energy minimum at the phase domain should be expected if the particle selectivity is sufficiently strong just the like the case of a small particle with flexible chains at $N\chi_P = -6.0$ (see Fig. 5a). In this situation, the particle staying at the domain center turns to be stable. The change of free energy with increasing the strength of particle selectivity is controlled mainly by the change of enthalpy, as the entropy is almost independent of the particle selectivity for both flexible and semiflexible chains. This is an implication that the particle interaction has little effect tuning the system entropy, especially for semiflexible chain systems with a small or large particle involved. Anyway, the profiles in Fig. 6 clearly illustrate that in the case of a large particle, the introduction of particle selectivity does not change the feature of particle distributions.

The analysis of enthalpy and entropy profiles for the case of a large particle in the system also supports the main conclusions obtained before for flexible chains, *i.e.*, the particle distribution in the domain center is determined by the enthalpy, while that for semiflexible chains, it is governed by the entropy. Indeed, for flexible chains, the profiles of entropy presented in Fig. 6(c) is nearly flat around $y_P/D_0 = -0.25$, so the enthalpy minimum appear there is responsible for the free energy minimum shown in each profile of Fig. 6. In contrast, for both moderately semiflexible and strongly semiflexible chains, the enthalpy is close to uniform that the shape of the free energy profile around $y_P/D_0 = -0.25$ is dominated by the distribution of entropy where it is significantly humped. These results reveal that the entropic effect in tuning the particle distribution in the particle-semiflexible chain composites is general irrelevant of the particle selectivity and particle size.

SUMMARY AND REMARKS

In this work, we investigate the effect of chain rigidity on the nanoparticle distribution when they are immersed in the lamellar morphology formed by semiflexible diblock copolymer chains, and in particular we focus on the influence on the metastable state appeared at the phase domain center. The SCF results show that the neutral particle generally prefers to stay at the interface, where it can reach a global free energy minimum. A metastable stable, *i.e.*, a local free energy minimum, at the phase domain center may appear depending on the chain rigidity and particle size. For example, in the case of flexible chains, we could find a quite weak free energy minimum at the domain center, and it becomes deep with the increase of particle size. In the case of moderately semiflexible chains, we find obvious free energy minimum at the domain center for both small and large particles. For strongly semiflexible chains, the free energy profile in the domain region has a close relation with the particle size, and a free energy minimum is observed

https://doi.org/10.1007/s10118-023-3053-9

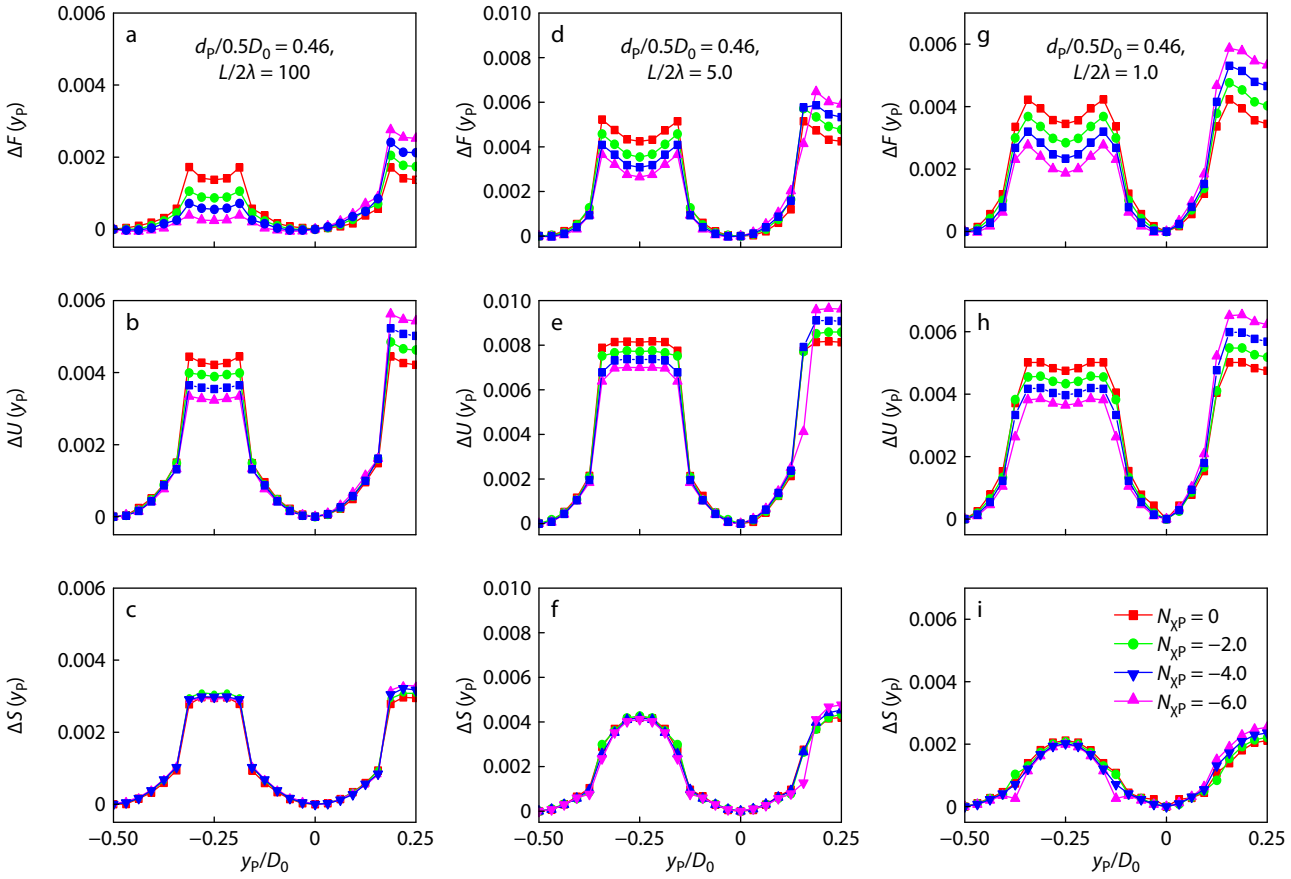

Fig. 6 The distribution of free energy, enthalpy and entropy for flexible chains $L/2\lambda = 100$ (a, b, c), moderately semiflexible chains $L/2\lambda = 5.0$ (d, e, f), and strongly semiflexible chains $L/2\lambda = 1$ (g, h, i) for a large particle with particle diameter $d_P/0.5D_0 = 0.46$. The particle selectivity is set as denoted, and $N_{\chi P} < 0$ means that the particle adsorbs B monomers and repels A monomers. The legends in (i) are identical and they refer to all other panels.

only when the particle is large. A typical consequence when the particle becomes selective is the decrease of free energy minimum at the domain center, and it turns to be a global minimum if the particle selectivity is sufficiently strong. In this case, the particle staying at the domain center becomes stable instead of that being at the interface. For neutral and weakly selective particles, at the domain center, only local minimums are observed, and this means that the particles staying at the domain centers still have large probability to move to the interface, and the waiting time depends on the chain rigidity as well as the strength of particle selectivity as have shown in our results.

Experiments investigating the nanoparticle distribution in the lamellar domains formed by flexible chains have been performed.[52,53] They all found strong dependence of the particle distribution on the particle size. For example, Thompson *et al.*[53] found that when $d_p/0.5D_0 < 0.6$, particles prefer to stay at the interface, while they tend to aggregate in the middle of the phase domain when $d_p/0.5D_0 > 0.6$. Bockstaller *et al.*[52] observed a different boundary value of $d_p/0.5D_0 \simeq 0.12$ separating these two different states of particle distributions. In our case for neutral particles, we only found metastable states at the domain center even when $d_p/0.5D_0 = 0.46$. A global minimum at the domain center may be observed when d_p is much larger. However, this is not considered in the present work because of the convergent problems solving the SCF equations. On the other hand, few experimental studies have been noticed focusing on the distribution of nanoparticles in microphases formed by self-assembly of semiflexible diblock copolymers, and therefore further experimental verification is highly desirable.

The split of the free energy into contributions from enthalpy and entropy reveals the underlying mechanisms that control the free energy profiles and thus the particle distributions at the phase domain. For flexible chains, it is the enthalpy that determines the subtle shape of the free energy profile at the phase domain, because the entropy there is nearly a particle position independent constant. Such entropic behavior arises from the flexible nature of polymer chains that the chain bonds near the free end can rotate themselves freely in response to the surrounding conditions such that the polymer chain is not compressed or stretched at all. On the other hand, for semiflexible chains, the entropy dominates the free energy distribution at the phase domain as the enthalpy there is more close to flat compared to that of the entropy. However, when the polymer chains are strongly semiflexible, the entropic behaviors differ from the particle size. In the case of a small particle, the minimum entropy tends to push the particle away from the domain center, and for a large particle, the maximum entropy tries to arrest the parti-

https://doi.org/10.1007/s10118-023-3053-9

cle at the domain center. The analysis of the chain conformations with the assistance of free end distribution demonstrates that the entropic behavior is in close relation with the way that the particle disturbs the semiflexible chain conformations. The introduction of particle selectivity does not change the picture for the enthalpy and entropy in affecting the particle distributions in the lamellar phase.

Our study specifies the significance of chain rigidity in determining the particle distributions in the lamellar phase. By exploiting the chain rigidity, one may find a facile way tuning the particle position on demand in the lamellar phase. For example, to remove small particles from the domain center, one could introduce an external electric or magnetic field to increase the rigidity of the polymer chain. The reversible occupation of the phase domain by particles may be explored for the design of some particle switch channels. In all, the chain rigidity and the induced entropic effect enrich the phase behaviors of the particle-polymer composites and may also leads to useful applications.

Conflict of Interests

The authors declare no interest conflict.

ACKNOWLEDGMENTS

This work was financially supported by the National Natural Science Foundation of China (No. 22173002). S.Q. acknowledges the Fundamental Research Funds for the Central Universities (No. YWF-22-K-101). J.Y. acknowledges the Fundamental Research Funds for the Central Universities from Beihang University. The SCF calculations were carried out on the high performance computer cluster at Beihang University.

REFERENCES

1 Al-Saleh, M. H. Influence of polymer structure on the electrical resistivity of nanocomposite materials. *Synth. Met.* **2020**, *256*, 116409.
2 Yang, Y.; He, J. L.; Li, Q.; Gao, L.; Hu, J.; Zeng, R.; Qin, J.; Wang, S. X.; Wang, Q. Self-healing of electrical damage in polymers using superparamagnetic nanoparticles. *Nat. Nanotechnol.* **2018**, *14*, 151–155.
3 Huang, Y.; Ellingford, C.; Bowen, C.; McNally, T.; Wu, D.; Wan, C. Y. Tailoring the electrical and thermal conductivity of multi-component and multi-phase polymer composites. *Int. Mater. Rev.* **2019**, *65*, 129–163.
4 Bockstaller, M. R.; Thomas, E. L. Proximity effects in self-organized binary particle-block copolymer blends. *Phys. Rev. Lett.* **2004**, *93*, 166106.
5 Wang, Y.; Liu, X.; Li, S.; Li, T.; Song, Y.; Li, Z.; Zhang, W.; Sun, J. Transparent, healable elastomers with high mechanical strength and elasticity derived from hydrogen-bonded polymer complexes. *ACS Appl. Mater. Interfaces* **2017**, *9*, 29120–29129.
6 Yang, Q.; Ye, C.; Zhao, J.; Chen, D.; Weng, B.; You, J.; Li, Y. Shape memory polymers with interconnected nanopores and high mechanical strength. *J. Polym. Sci., Part B: Polym. Chem.* **2017**, *56*, 125–130.
7 Sharma, U.; Concagh, D.; Core, L.; Kuang, Y.; You, C.; Pham, Q.; Zugates, G.; Busold, R.; Webber, S.; Merlo, J.; Langer, R.; Whitesides, G. M.; Palasis, M. The development of bioresorbable composite polymeric implants with high mechanical strength. *Nat. Mater.* **2017**, *17*, 96–103.
8 Bosquetti, M.; da Silva, A. L.; Azevedo, E. C.; Berti, L. F. Analysis of the mechanical strength of polymeric composites reinforced with sisal fibers. *J. Nat. Fibers* **2019**, *18*, 105–110.
9 Zhao, X.; Liu, J.; Li, J.; Liang, Z.; Zhou, W.; Peng, S. Strategies and techniques for improving heat resistance and mechanical performances of poly(lactic acid) (PLA) biodegradable materials. *Int. J. Biol. Macromol.* **2022**, *218*, 115–134.
10 Peelman, N.; Ragaert, P.; Ragaert, K.; Erkoç, M.; Brempt, W. V.; Faelens, F.; Devlieghere, F.; Meulenaer, B. D.; Cardon, L. Heat resistance of biobased materials, evaluation and effect of processing techniques and additives. *Polym. Eng. Sci.* **2017**, *58*, 513–520.
11 Ozerin, S. A.; Vdovichenko, A. Y.; Streltsov, D. R.; Davydov, A. B.; Orekhov, A. S.; Vasiliev, A. L.; Zubavichus, Y. V.; Grigoriev, E. I.; Zavyalov, S. A.; Oveshnikov, L. N.; Aronzon B. A.; Chvalun, S. N. Structure and magnetic properties of Ni-poly(*p*-xylylene) nanocomposites synthesized by vapor deposition polymerization. *J. Phys. Chem. Solids* **2017**, *111*, 245–253.
12 Barrera, G.; Tiberto, P.; Allia, P.; Bonelli, B.; Esposito, S.; Marocco, A.; Pansini, M.; Leterrier, Y. Magnetic properties of nanocomposites. *Appl. Sci.* **2019**, *9*, 212.
13 Sanida, A.; Stavropoulos, S. G.; Speliotis, T.; Psarras, G. C. Investigating the effect of Zn ferrite nanoparticles on the thermomechanical, dielectric and magnetic properties of polymer nanocomposites. *Materials* **2019**, *9*, 3015.
14 Balazs, A. C.; Emrick, T.; Russell, T. P. Nanoparticle polymer composites: where two small worlds meet. *Science* **2006**, *314*, 1107–1110.
15 Harijan, M.; Singh, M. Zwitterionic polymers in drug delivery: A review. *J. Mol. Recognit.* **2021**, *35*, e2944.
16 Li, M.; Zhang, W.; Li, J.; Qi, Y.; Peng, C.; Wang, N.; Fan, H.; Li, Y. Zwitterionic polymers: addressing the barriers for drug delivery. *Chin. Chem. Lett.* **2023**, 108177.
17 Fu, X.; Hosta-Rigau, L.; Chandrawati, R.; Cui, J. Multi-stimuli-responsive polymer particles, films, and hydrogels for drug delivery. *Chem* **2018**, *4*, 2084–2107.
18 Kolate, A.; Baradia, D.; Patil, S.; Vhora, I.; Kore, G.; Misra, A. PEG — A versatile conjugating ligand for drugs and drug delivery systems. *J. Control. Rel.* **2014**, *192*, 67–81.
19 Jeon, S. J.; Yang, S. M.; Kim, B. J.; Petrie, J. D.; Jang, S. G.; Kramer, E. J.; Pine, D. J.; Yi, G. R. Hierarchically structured colloids of diblock copolymers and Au nanoparticles. *Chem. Mater.* **2009**, *21*, 3739–3741.
20 Nuopponen, M.; Tenhu, H. Gold nanoparticles protected with pH and temperature-sensitive diblock copolymers. *Langmuir* **2007**, *23*, 5352–5357.
21 Kim, B. J.; Fredrickson, G. H.; Hawker, C. J.; Kramer, E. J. Nanoparticle surfactants as a route to bicontinuous block copolymer morphologies. *Langmuir* **2007**, *23*, 7804–7809.
22 Jang, J.; Li, X. L.; Oh, J. H. Facile fabrication of polymer and carbon nanocapsules using polypyrrole core/shell nanomaterials. *Chem. Commun.* **2004**, 794.
23 Hamdoun, B.; Ausserré, D.; Joly, S.; Gallot, Y.; Cabuil, V.; Clinard, C. New nanocomposite materials. *Journal de Physique II* **1996**, *6*, 493–501.
24 Lauter-Pasyuk, V.; Lauter, H. J.; Ausserre, D.; Gallot,Y.; Cabuil, V.; Hamdoun, B.; Kornilov, E. I. Neutron reflectivity studies of composite nanoparticle – copolymer thin films. *Phys. B Condens. Matter* **1998**, *248*, 243–245.
25 Dong, B.; Guo, R.; Yan, L. T. Coassembly of Janus nanoparticles in asymmetric diblock copolymer scaffolds: unconventional entropy effect and role of interfacial topology. *Macromolecules*

2014, *47*, 4369–4379.
26 Tabedzki, C.; Krook, N. M.; Murray, C. B.; Composto, R. J.; Riggleman, R. A. Effect of graft length and matrix molecular weight on string assembly of aligned nanoplates in a lamellar diblock copolymer. *Macromolecules* **2022**, *55*, 3166–3175.
27 Aviv, Y.; Altay, E.; Fink, L.; Raviv, U.; Rzayev, J.; Shenhar, R. Quasi-two-dimensional assembly of bottlebrush block copolymers with nanoparticles in ultrathin films: combined effect of graft asymmetry and nanoparticle size. *Macromolecules* **2018**, *52*, 196–207.
28 Hamley, I. W. *Developments in block copolymer science and technology*, Wiley, New York, **2004**.
29 Bates, F. S. Block copolymers – designer soft materials. *Physics Today* **1999**, *52*, 32–38.
30 Bates, F. S.; Hillmyer, M. A.; Lodge, T. P.; Bates, C. M.; Delaney, K. T.; Fredrickson, G. H. Multiblock polymers: Panacea or Pandora's box? *Science* **2012**, *336*, 434–440.
31 Leibler, L. Theory of microphase separation in block copolymers. *Macromolecules* **1980**, *13*, 1602–1617.
32 Chiu, J. J.; Kim, B. J.; Kramer, E. J.; Pine, D. J. Control of nanoparticle location in block copolymers. *J. Am. Chem. Soc.* **2005**, *127*, 5036–5037.
33 Gu, J.; Zhang, R.; Zhang, L.; Lin, J. Epitaxial assembly of nanoparticles in a diblock copolymer matrix: precise organization of individual nanoparticles into regular arrays. *Macromolecules* **2021**, *54*, 2561–2573.
34 Bockstaller, M. R.; Mickiewicz, R. A.; Thomas, E. L. Block copolymer nanocomposites: perspectives for tailored functional materials. *Adv. Mater.* **2005**, *17*, 1331–1349.
35 Zhang, L.; Lin, J.; Lin, S. Self-Assembly behavior of amphiphilic block copolymer/Nanoparticle mixture in dilute solution studied by self-consistent-field theory/density functional theory. *Macromolecules* **2007**, *40*, 5582–5592.
36 Jin, J.; Wu, J.; Frischknecht, A. L. Modeling microscopic morphology and mechanical properties of block copolymer/nanoparticle composites. *Macromolecules* **2009**, *42*, 7537–7544.
37 Lindsay, B. J.; Composto, R. J.; Riggleman, R. A. Equilibrium field theoretic study of nanoparticle interactions in diblock copolymer melts. *J. Phys. Chem. B* **2019**, *123*, 9466–9480.
38 Matsen, M. W.; Thompson, R. B. Particle Distributions in a block copolymer nanocomposite. *Macromolecules* **2008**, *41*, 1853–1860.
39 Jiang, Y.; Zhang, W. Y.; Chen, J. Z. Y. Dependence of the disorder-lamellar stability boundary of a melt of asymmetric wormlike *AB* diblock copolymers on the chain rigidity. *Phys. Rev. E* **2011**, *84*, 041803.
40 Jiang, Y.; Chen, J. Z. Y. Influence of chain rigidity on the phase behavior of wormlike diblock copolymers. *Phys. Rev. Lett.* **2013**, *110*, 138305.
41 Uchida, K.; Mita, K.; Yamamoto, S.; Tanaka, K. Local orientation of polystyrene at the interface with poly(methyl methacrylate) in block copolymer. *ACS Macro Lett.* **2020**, *9*, 1576–1581.
42 Aldaye, F. A.; Palmer, A. L.; Sleiman, H. F. Assembling materials with DNA as the guide. *Science* **2008**, *321*, 1795–1799.
43 Zhou, C.; Duan, X.; Liu, N. DNA-nanotechnology-enabled chiral plasmonics: from static to dynamic. *Acc. Chem. Res.* **2017**, *50*, 2906–2914.
44 Spakowitz, A. J.; Wang, Z. G. End-to-end distance vector distribution with fixed end orientations for the wormlike chain model. *Phys. Rev. E* **2005**, *72*, 041802.
45 Kratky, O.; Porod, G. Röntgenuntersuchung gelöster Fadenmoleküle. *Recueil des Travaux Chimiques des Pays-Bas* **1949**, *68*, 1106–1122.
46 Saitô, N.; Takahashi, K.; Yunoki, Y. The statistical mechanical theory of Stiff chains. *J. Phys. Soc. Jpn.* **1967**, *22*, 219–226.
47 Chen, Y.; Zhang, X.; Jiang, Y. The influence of side-chain conformations on the phase behavior of bottlebrush block polymers. *Soft Matter* **2020**, *16*, 8047–8056.
48 Matsen, M. W. Melts of semiflexible diblock copolymer. *J. Chem. Phys.* **1996**, *104*, 7758–7764.
49 Vorselaars, B.; Kim, J. U.; Chantawansri, T. L.; Fredrickson G. H.; Matsen, M. W. Self-consistent field theory for diblock copolymers grafted to a sphere. *Soft Matter* **2011**, *7*, 5128–5137.
50 Thompson, R. B.; Rasmussen, K. O.; Lookman, T. Improved convergence in block copolymer self-consistent field theory by Anderson mixing. *J. Chem. Phys.* **2004**, *120*, 31–34.
51 Matsen, M. W. Fast and accurate SCFT calculations for periodic block-copolymer morphologies using the spectral method with Anderson mixing. *Eur. Phys. J. E* **2009**, *30*, 361.
52 Bockstaller, M. R.; Lapetnikov, Y.; Margel, S.; Thomas, E. L. Size-selective organization of enthalpic compatibilized nanocrystals in ternary block copolymer/particle mixtures. *J. Am. Chem. Soc.* **2003**, *125*, 5276–5277.
53 Thompson, R. B.; Ginzburg, V. V.; Matsen, M. W.; Balazs, A. C. Predicting the mesophases of copolymer-nanoparticle composites. *Science* **2001**, *292*, 2469–2472.

https://doi.org/10.1007/s10118-023-3053-9